Quantum Electronics **33** (1) 37 – 44 (2003)

PACS numbers: 42.55.Lt; 42.60.Lh; 71.35.-y
DOI: 10.1070/QE2003v033n01ABEH002362

Liquid xenon excimer laser

A.G. Molchanov

***Abstract*. The characteristics of the first excimer laser and the history of its creation are presented. The threshold lasing conditions and the modern theory of active media are considered, and the prospects for the development of excimer lasers operating on condensed rare gases are discussed. It is shown that in experiments on pumping liquid xenon, lasing was obtained simultaneously on excimers of several types, including excimers in liquid and gas phases.**

Keywords: *excimer, excimer lasers, self-trapped excitons, rare-gas crystals.*

1. Introduction

The history of creation of excimer lasers is an example of how unpredictable can be sometimes the route from an original idea to its practical implementation. The author of this paper conceived the idea of using rare gas crystals to obtain lasing on the interband or excitonic transitions in 1964 during the post-gradual theoretical study of the properties of excitons in molecular crystals (it is rare-gas crystals that were used as a model for introducing the concept of excitons [1]), which he performed under the supervision of V.L. Ginzburg at the P.N. Lebedev Physics Institute (FIAN). The author introduced this idea to V.A. Danilychev, who studied the electronic excitation of semiconductors at N.G. Basov's laboratory. N.G. Basov appreciated at once the importance of a new promising research field, first of all from the point of view of the development of semiconductor lasers emitting in the VUV spectral region, and included this topic to the studies performed at his Laboratory of Quantum Radiophysics at FIAN.

By opening the IV International Conference on Quantum Electronics, N.G. Basov informed about the purpose to obtain lasing in condensed rare gases in the VUV region at the Laboratory of Quantum Radiophysics. This statement contained only two sentences: 'Attempts are being made to use noble gases at low temperatures as the working media to obtain emission in the region of the far vacuum ultraviolet. According to preliminary estimates, in spite of the broad linewidths due mainly to exchanger interaction, one can expect here a narrow emission line similar to the case of semiconductors, since the collective excitation of atoms at low temperature would be concentrated near the edge of the line' [2].

The words 'the collective excitation of atoms' and 'one can expect here a narrow emission line similar to the case of semiconductors' meant at that time that lasing was expected on the transitions of free excitons with emission of phonons, as occurred in CdS crystals at liquid nitrogen temperature [3].

By preparing together with V.A. Danilychev the report for this conference concerning rare-gas crystals, the author, who became a staff member of the Laboratory of Quantum Radiophysics in 1965, suggested to N.G. Basov to show the band structure of crystalline xenon at the conference. However, N.G. Basov, who intuitively understood that a general trend of the research was important rather than its details, declined this proposal. Indeed, it was found soon that neither the band structure nor collective excitations of free excitons play any substantial role. It should be noted that excimer transitions were never mentioned until this time. At the end of 1966, the author came across the paper on luminescence of condensed rare gases excited by alpha particles [4]. The luminescence bands observed in the condensed phase in this paper coincided with the luminescence bands of molecules of rare gases. As a result, it become obvious to the author that lasing should be expected not on the transitions of free excitons but first of all on the transitions of excimers, which are usually called in rare-gas crystals and alkali halide crystals the localised or self-trapped excitons.

The threshold of lasing on the excimer transitions in condensed rare gases pumped by a fast-electron beam was calculated for the first time in paper [5]. It turned out that typical threshold specific pump powers should be ~ 100 MW cm^{-3}. Such high specific pump powers are typical for semiconductor lasers, and they became attainable first of all due to the development in the mid-1960s of the method for pumping these lasers by a fast-electron beam. It was also pointed out in [5] that the active medium of excimer lasers exhibits two specific features: an increase in absorption with increasing pump power and a very high efficiency of energy transfer from rare gases to impurities, as well as the possibility of lasing in mixtures. In 1969, the amplification of excimer emission was first observed at the Laboratory of Quantum Radiophysics at FIAN upon excitation of liquid xenon by a fast-electron beam [6].

A.G. Molchanov P.N. Lebedev Physics Institute, Russian Academy of Sciences, Leninskii prosp. 53, 119991 Moscow, Russia; e-mail: molchan@sci.lebedev.ru

Received 23 September 2002
Kvantovaya Elektronika **33** (1) 37 – 44 (2003)
Translated by M.N. Sapozhnikov

The amplification was detected at a wavelength of 175 nm by observing the narrowing of the emission spectrum. The passage from amplification [6–8] to lasing, which was first observed in 1970 [9], was achieved by increasing the electron-beam power by an order of magnitude. The distinct lasing on excimer transitions was observed in Ref. [10] on the same setup as in [9]. In this case, the angular directivity diagram narrowed down to 3°, and the far-field interference pattern was observed, indicating to coherent radiation. In [11], the theory of the energy level diagram of excimers in rare-gas crystals was developed in a close relation with experiments, which explained the mechanism of luminescence and lasing in condensed rare gases.

The similarity between excimers in condensed and gas phases and the possibility of lasing on excimer transitions in compressed rare gases upon electron excitation were pointed out in review [12] published at the beginning of 1972. The lasing was obtained in gaseous xenon at the Lawrence Livermore Laboratory (USA) in June 1972 [13]. It was reported in this paper and subsequent papers [14–16], referring to [5, 9], that the lasing efficiency in gases and the emission spectrum proved to be almost the same as those observed in [9] upon the electron-beam pumping of liquid xenon. Lasing of excimers was later observed in condensed rare gases in papers [17–21].

The reasonable question arises why lasing was not obtained on the excimer transitions in rare gases immediately after the publication of paper [22], where the possibility of using $Ar_2^*, Kr_2^*, Xe_2^*, Hg_2^*$ etc. molecules for this purpose was pointed out. The answer is probably that, unlike [5], the author of [22] did not calculate the threshold pump intensity, which proved to be for these lasers many orders of magnitude greater than the threshold intensities of gas lasers available at that time. This is evidenced by the unsuccessful attempts to obtain excimer lasing in a usual electric discharge [23] using the specific pump power of the order of 1 W cm^{-3}. The broad emission bands of excimers (their width is sometimes three order of magnitudes greater than the Doppler width) and a short emission wavelength, which lies in the VUV spectral region for the simplest excimers in rare gases, result in the high threshold specific pump powers for these lasers, exceeding hundreds of kilowatts per cubic centimetre. Such high specific powers became attainable only in the mid-1960s due to the use of fast-electron beams for pumping semiconductor lasers. A drastic increase in the specific power of electric discharges was achieved in 1971 by using volume discharges with an external preionisation to excite CO_2 lasers. Therefore, the creation of the first excimer laser based namely on liquid xenon was caused, on the one hand, by the natural advancement of semiconductor lasers to the wide energy-gap materials and, on the other hand, by the existence of high-power sources at that time for their pump.

It is shown below, based on the analysis of the emission spectra and calculations of the output radiation intensity, that in experiments on pumping liquid xenon, lasing was observed simultaneously for several types of excimers, including excimers in liquid and gas phases. The theory of the active medium of a condensed xenon excimer laser presented below is based on the modern concepts about processes proceeding in condensed rare gases at high excitation intensities.

2. Energy level diagram and the laser transition in liquid xenon

The similarity of the excimer luminescence bands of rare gases in condensed and gas phases [4] gives the illusion that the luminescence spectra of rare-gas crystals can be interpreted using the energy level diagram of free molecules. However, the absorption spectra of rare-gas crystals exhibiting two hydrogen-like series of levels of free excitons $\Gamma(3/2)$ and $\Gamma(1/2)$, which are absent in the gas phase, demonstrate that this is not the case. Fig. 1 shows the absorption spectrum of crystalline xenon, which distinctly displays both these series. At the top, the positions of the lower atomic lines $^3P_1$ and $^1P_1$, and the ionisation potential $I_{Xe} = 12.1$ eV are shown. The ionisation potential in the crystal corresponds to the limit (9.28 eV) of the lower hydrogen-like series of the exciton levels $\Gamma(3/2)$, which is smaller than the ionisation potential in the gaseous xenon almost by 3 eV. The energy levels of free excitons for the lower series are quite well described by the expression

$$E_n = E_g - \frac{\mu}{\varepsilon_0^2}\frac{I_H}{n^2}, \quad n = 1, 2, 3, ..., \tag{1}$$

where $E_g = 9.28$ eV is the energy gap; $\mu = 0.31$ is the effective mass of the exciton (in units of the electron mass); $\varepsilon_0 = 2.23$ is the dielectric constant of the crystal; and $I_H = 13.6$ eV is the ionisation potential of hydrogen. Upon localisation of free electrons in a crystal lattice, their energy levels should transform to the corresponding potential curves of excimers, which do not coincide, of course, with the potential curves of free molecules. In addition, the symmetry group D_{2h} of a self-trapped exciton does not coincide with the symmetry group D_h of the rare-gas molecule, and the number of energy levels and their classification in the condensed and gas phases will be different.

To calculate the energy level diagram of self-trapped excitons and to find the relation between the absorption and

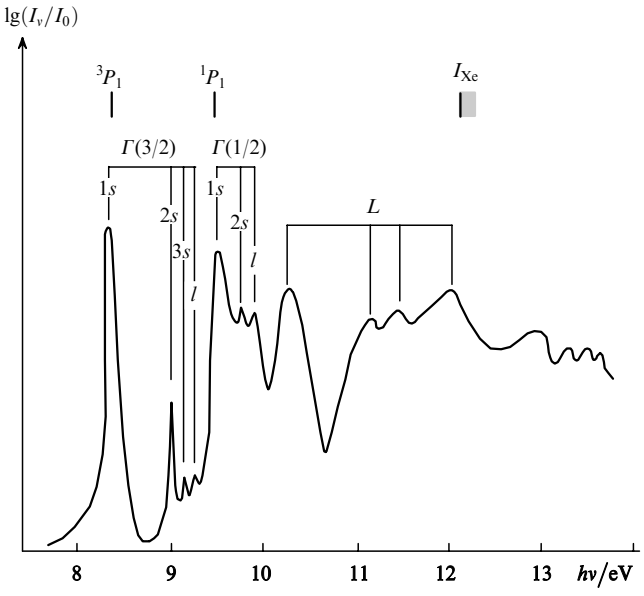

Figure 1. Absorption spectrum of crystalline xenon at 21 K [24].

luminescence spectra of condensed rare gases, a group-theoretic analysis of the energy level diagrams of self-trapped excitons, diatomic molecules, atoms, and free excitons was performed in paper [11]. This analysis made it possible to classify the energy levels of self-trapped excitons in condensed rare gases and to relate them with the energy levels of diatomic molecules. The potential curves of self-trapped excitons were calculated in [11] by the pseudopotential method, taking the Rydberg type of levels explicitly into account. The calculations showed that each of the two hydrogen-like series $\Gamma(3/2)$ and $\Gamma(1/2)$ of the energy levels of free excitons consists in turn of two series: the first one, which is dipole allowed, and the second (with a lower energy) forbidden series, which is not observed in the absorption spectra. It was found that upon deformation of the crystal lattice, a partially allowed series of the energy levels of self-trapped excitons splits from the levels of the second forbidden series. Thus, it was shown that the energy levels of self-trapped excitons in rare-gas crystals form two principal hydrogen-like series, which were called the σ and π series, according to the polarisation of their radiation (Fig. 2).

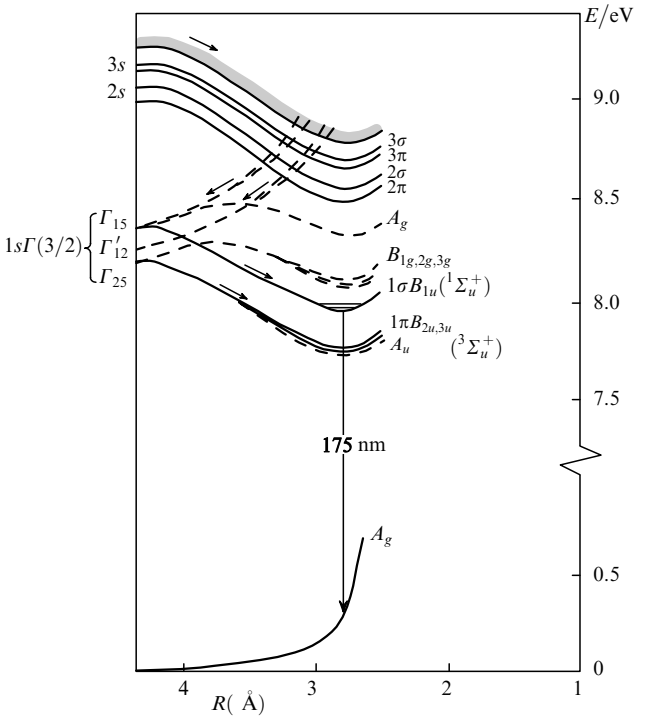

Figure 2. Potential curves of excimers and the laser transition in condensed xenon.

The lifetime of the lower, partially allowed triplet 1π level in xenon proved to be an order of magnitude (in other rare gases, a few orders of magnitude) longer than that of the upper 1σ level. The results obtained for rare-gas crystals are qualitatively the same for the liquid state because of the conservation of the short-range-order symmetry. It followed from this, in particular, that generation in the first liquid xenon laser occurred mainly from the 1σ level, whereas the lower 1π level served as the energy reservoir. This result (using the appropriate notation of the energy levels) proved to be valid for all excimer lasers operating on rare gases. Lasing in them occurs upon transitions to the lower repulsive level not from the lowest metastable excimer level but from the allowed level located above the metastable level. Note, however, that rare gases in the condensed state retain some optical properties of the gas phase. The positions of the lower atomic lines $^3P_1$ and $^1P_1$ in the absorption spectra almost coincide with the lower excitonic absorption peaks, while the luminescence bands in the condensed and gas phases overlap with each other. This dualism of the optical properties of rare gases, as will be shown below, has played an unexpected role in the generation obtained in the first excimer laser.

3. Threshold lasing conditions for excimer emission

The rate W^+ of producing electron–hole pairs in condensed xenon irradiated by a fast-electron beam is described by the expression

$$W^+ = \frac{W_b}{I_i} = \frac{j_b}{e I_i}\left(\frac{dE}{dx}\right)_{eff}, \quad (2)$$

where W_b is the specific pump power; $I_i = 15.6$ eV is the energy spent for producing one electron–hole pair [25]; and j_b is the electron-beam current density. The effective stopping power of any material is related to the initial electron energy E_0 in the beam by the expression [26]

$$\left(\frac{dE}{dx}\right)_{eff} = \frac{E_0}{0.4\,x_r}, \; x_r = \frac{137^4}{24\pi a_H^2 N_A \rho}\frac{A}{Z}\frac{E_0^2}{mc^2(mc^2+E_0)}, \quad (3)$$

where x_r is the maximum range of an electron; ρ is the material density; A/Z is the ratio of the atomic weight of the element to its number; a_H is the Bohr radius; and N_A is Avogadro's number. In liquid xenon ($\rho = 3.1$ g cm^{-3}, $A/Z = 2.43$) , the maximum range for the electron beam with the energy $E_0 = 0.6$ MeV is $x_r = 0.12$ cm, the effective excitation depth is $x_0 = 0.4x_r = 0.05$ cm, and the specific power $W_b = E_0 j_b/(e x_0)$ is 12 MW cm^{-3} when the current density is $j_b = 1$ A cm^{-2}. The simplest lasing threshold condition for a resonator with plane mirrors has the form [5, 10]

$$g_0 \geqslant a_i - \frac{\ln(R_1 R_2)}{2L}, \quad (4)$$

where R_1 and R_2 are the reflection coefficients of the mirrors; L is the length of the resonator filled with an active medium; g_0 and a_i are the unsaturated gain and internal absorption coefficient, respectively. By taking the values of the cross section for stimulated transition $\sigma_0 = 1.5 \times 10^{-17}$ cm^2, the spontaneous lifetime of the upper laser level $\tau_s = 2.2 \times 10^{-9}$ s, and the quantum efficiency of emission $\eta_s = 0.5$, which are used at present [20, 21, 27], we obtain that the threshold current density for the first excimer laser with the absorption coefficient $a_i = 0.15$ cm^{-1}, the resonator length $L = 1$ cm, and the reflection coefficients $R_1 = R_2 = 0.5$ should be roughly 10 A cm^{-2}. It is shown below that more accurate calculations give the value of 25 A cm^{-2}, which corresponds to the experimental data: for $j_b = 30$ A cm^{-2}, the emission line was narrowed down by 30 % [6], while for $j_b = 150$ A cm^{-2}, high-level excimer lasing was observed [9, 10].

Fig. 3 shows the emission spectra of xenon for different currents of electron-beam pump. These spectra are taken

from paper [9] and were demonstrated by the author at the International Conference on Luminescence in 1972 [10]. Along with the central 175-nm band corresponding to lasing of xenon excimers in liquid, the spectra also exhibited the 172-nm band, whose intensity was two times lower, which belonged to the emission of Xe_2^* excimers in gas. The authors of papers [9, 10] did not ponder at that time whether the 172-nm band corresponded to excimer lasing achieved also in gaseous xenon.

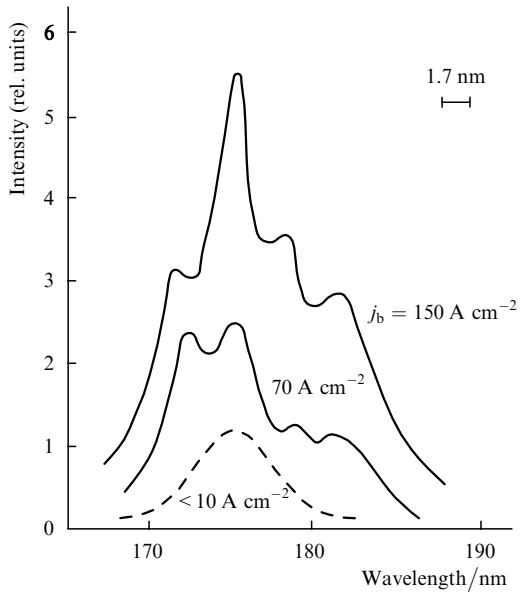

Figure 3. Emission spectra observed upon pumping of liquid xenon by a 10-ns, 600-keV electron beam in a resonator with plane mirrors ($R_1 = R_2 = 0.5$) for different beam-current densities. The spectrometer resolution is 1.7 nm.

At present, we can say certainly that the pump powers used in these experiments were sufficient to boil up the surface layer of liquid xenon and to achieve excimer lasing simultaneously in liquid xenon and the gaseous xenon layer near the liquid surface. In any case, the output lasing power was so high that at the current density $j_b = 150$ A cm^{-2} the aluminium mirrors used in the experiments were burnt out according to the form of a laser beam spot after one–two shots of an electron gun. V.A. Danilychev demonstrated these mirrors many times to the author. Taking into account the relation between the intensities of emission bands in Fig. 3 and using the calculations presented below, it is safe to say that the lasing observed in 1970 at N.G. Basov's laboratory occurred simultaneously in excimers of several types, including Xe_2^* excimers in gas. This could not have happened if the experiments had been performed with crystalline xenon.

The lasing spectrum exhibits also two less intense bands to the red from the central 175-nm band at 178.5 and 182 nm (Fig. 3). The 178.5-nm band can be assigned to lasing of 1π excimers because the difference between the energies of photons corresponding to the wavelengths 175 and 178.5 nm is equal to the distance between the energy levels of 1σ and 1π excimers. In addition, the lifetime of 1π excimers in condensed xenon is only an order of magnitude shorter than that of 1σ excimers, whereas the statistical weight of the former is three times larger. For this reason, the gain in 1π excimers upon intense pumping can be only three times lower that that in 1σ excimers, which is quite sufficient to obtain lasing on triplet excimers. The 182-nm band is probably caused by contribution to the lasing from the second vibrational level of the 1σ excimer or by lasing of impurities.

The experiments were performed with liquid xenon rather than with crystalline xenon because the absorption coefficient in liquid is lower than that in the crystal. Absorption at 175 nm in a crystalline xenon was 0.5 cm^{-1} in the best case, whereas it was only 0.15 cm^{-1} in liquid. In addition, no defects were accumulated in liquid xenon irradiated by an electron beam, whereas such defects were observed in a crystalline xenon.

4. Kinetics and output characteristics of a liquid xenon excimer laser

Under the action of a fast-electron beam, electron–hole pairs and free excitons are produced in condensed xenon. Free holes, which we will denote as H_1, are transformed during self-trapping to self-trapped holes H_2, whose structure is close to that of a molecular xenon ion. The kinetics of excimer luminescence and lasing in liquid xenon is manly determined by transitions from the lower singlet and triplet levels of free (S_1, T_1) and self-trapped (S_2, T_2) excitons (Fig. 4). Free excitons S_1 and T_1 are formed in the dissociative recombination of electrons and self-trapped holes. The energy levels T_1 and S_1 of free excitons and of holes (H_1) in a crystalline xenon are 8.26, 8.38, and 9.28 eV, and the minima of potential curves of self-trapped excitons T_2 and S_2 and holes H_2 are 7.64, 7.76, and 8.78 eV, respectively.

The pump rate W^* of the lower level of a free exciton by an electron beam is related to the rate (2) of producing electron–hole pairs by the expression

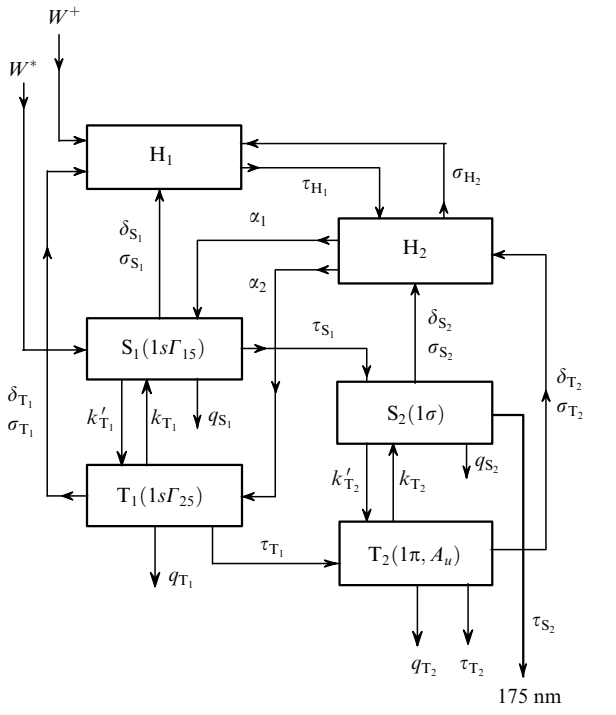

Figure 4. Scheme of kinetic processes in the active medium of a liquid xenon excimer laser excited by a fast-electron beam.

$$W^* = \eta_{ex} W^+, \quad (5)$$

where $\eta_{ex} = 0.06$ [23]. Most rate constants of the processes controlling the concentrations of electrons and excitons were taken from papers [18–21, 25], except the cross sections for ionisation of excitons by electron impact and the cross sections for transitions between triplet and singlet excitons. These cross sections were approximated by the expression [26]

$$Q_j(\varepsilon) = Q_j^m \alpha^\alpha \left(\frac{\varepsilon_j}{\alpha - 1}\right)^{\alpha-1} \frac{\varepsilon - \varepsilon_j}{\varepsilon^\alpha}, \quad (6)$$

where ε is the electron energy. In (6), the values of a constant α and the maximum cross section Q_j^m for atomic xenon were used and the corresponding exciton energy as the threshold energy ε_j of the jth inelastic process.

In the case of the Maxwell distribution of electrons, the rate constants (in cm ^{3} s^{-1}) of reactions can be written in the analytic form

$$k_j(T_e) = \langle v Q_j \rangle = 6.7 \times 10^{-9} \varepsilon_j Q_j^m \times \frac{\alpha^\alpha}{(\alpha-1)^{\alpha-1}} \frac{[\varepsilon_j/(k_B T_e)]^{\alpha-2/3}}{1 + [\varepsilon_j/(k_B T_e)]^{\alpha-1}} \exp[-\varepsilon_j/(k_B T_e)]. \quad (7)$$

The principle of detailed balancing gives the rate constant of the inverse process

$$k'_j(T_e) = k_j(T_e) \exp[-\varepsilon_j/(k_B T_e)]. \quad (8)$$

In addition, we will calculate not only the electron concentration, as in [20], but also the concentrations of free and self-trapped holes because the latter can be the centres of optical absorption and can affect the temperature dependence of the laser radiation intensity. This is all the more important for condensed xenon because the rate constant of dissociative recombination in it is two orders of magnitude lower than that in gas, so that the concentration of self-trapped holes can be very high. We will calculate the temperature of condensed xenon from the overall input energy deposited by an electron beam, without considering the contributions from each of the processes, as in [20]. Such a detailed treatment surely exceeds the accuracy of this model. The system of kinetic equations describing the active medium of the liquid xenon laser and the parameters of this system are presented in Appendix. Note only that the gain g and the unsaturated absorption coefficient a were calculated from the expressions

$$g = \sigma_0 n_{S_2}, \; a = a_i + \sigma_{S_1} n_{S_1} + \sigma_{T_1} n_{T_1} + \sigma_{T_2} n_{T_2} + \sigma_{H_2} n_{H_2}, \quad (9)$$

where, besides the distributed losses by impurities $a_i = 0.15$ cm^{-1}, the absorption by free excitons S_1 and T_1, self-trapped triplet excitons T_2, and self-trapped holes H_2 is taken into account; and σ_j and n_j are the absorption cross section and concentration of excitons and holes, respectively.

The saturating power density was calculated from the expression, which takes into account inelastic collisions of the working excimer S_2 with electrons and excitons:

$$I_s = \frac{h\nu}{\sigma_0} \left[\frac{1}{\tau_{S_2}} + (k'_{T_2} + \delta_{S_2} + q_{S_2}) n_e + \sum_j p_{S_2 j} n_j\right], \quad (10)$$

where $j = S_1, T_1, S_2, T_2$; n_e is the electron concentration; q_{S_2}, and k'_{T_2} are the quenching rate constants of the working excimer upon transitions to the ground and triplet states, respectively; δ_{S_2} is the rate constant of ionisation by electrons; and $p_{S_2 j}$ is the rate constant of ionisation (quenching) in collisions of the working excimer with other excimers and excitons.

In this paper, we calculated the output characteristics of a liquid xenon laser with parameters used in [9, 10], i.e., the reflectivities of mirrors $R_1 = R_2 = 0.5$, the active medium length $L = 1$ cm, the fast-electron beam energy 600 keV, and the current densities $j_b = 1 - 150$ A cm^{-2}. The pump pulse was rectangular, of duration 10 ns. The maximum current density of 150 A cm^{-2} corresponds to the specific pump power of 1800 MW cm^{-3} or the input specific pulse energy of 18 J cm^{-3}. Liquid xenon exists at normal pressure in the temperature range from 161.3 K (melting temperature) to 165.2 K (vaporisation temperature), i.e., within the range of 4 K. Therefore, at the specific input energy of 18 J cm^{-3}, neglecting the energy spent for sublimation, the temperature of liquid xenon should increase by 30 K, which is sufficient for its evaporation with excess. For conditions under study, the evaporation of xenon should begin at $j_b > 20$ A cm^{-2}, i.e., when the pump power exceeds the lasing threshold, as follows from calculations. To find the exact distributions of temperature and density of xenon near the surface, it is necessary to solve a complicated gas-dynamic problem, which takes into account the evaporation of the liquid and expansion of xenon vapours. Therefore, the equation for temperature used here gives only estimates and is valid, strictly speaking, only for condensed phase. In any case, the above estimates show that at the maximum current density, the intense sublimation of xenon occurs accompanied by the formation of a gaseous layer, which inevitably should be involved in excimer lasing.

Fig. 5 shows the dependences of the gain and the unsaturated absorption coefficient on the specific pump power calculated in the presence (g, a) and absence (g_0, a_0) of the field. The gain and the absorption coefficient were calculated

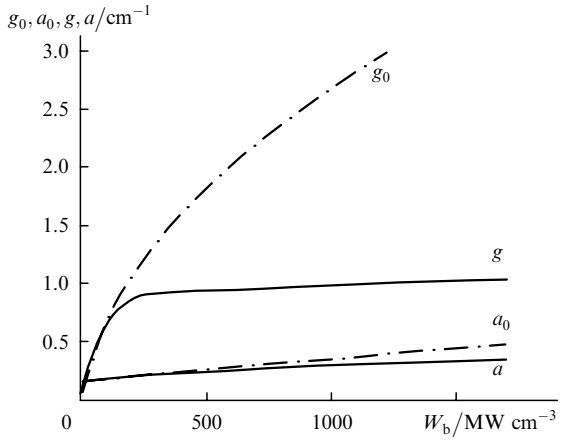

Figure 5. Dependences of the gain g and the absorption coefficient a on the specific pump power W_b in liquid xenon; g_0 and a_0 are the gain and the absorption coefficient in the absence of a field in the resonator.

at the instant $t = 10$ ns of the pulse end, when all the parameters acquired quasi-stationary values.

Fig. 6 shows the dependences of the output intensity I_{out}, the field intensity I in the cavity, and the saturating power density I_s on the specific pump power W_b calculated at the instant of the pulse end. One can see that a laser of this type has an interesting feature. Because I_s strongly increases with increasing W_b, the laser continues to operate in an unsaturated regime even at huge pump powers. This allows one to increase the active-region length and the output power by increasing W_b despite an increase in absorption. The lasing threshold (4) is achieved at $j_b = 25$ A cm^{-2}, which corresponds to $W_b = 280$ MW cm^{-3}, although the amplified spontaneous emission makes a noticeable contribution at the output already for $W_b > 100$ MW cm^{-3}. According to the calculation for the current density $j_b = 150$ A cm^{-2}, the maximum lasing efficiency relative to the input energy should be 20 % and the specific energy output should be 3.6 J cm^{-3}. For the specific pump power corresponding to $j_b = 150$ A cm^{-2}, the output intensity of the laser at 175 nm was 360 MW cm^{-2}. According to Fig. 3, the output intensity at 172 nm related to Xe_2^* excimers in the gas phase should be approximately less by half, being 170 MW cm^{-2}. It is interesting to note that for $j_b = 70$ A cm^{-2}, both lasing bands of xenon excimers in liquid and gas phases should have the same output power $I_{out} \approx 120$ MW cm^{-2}.

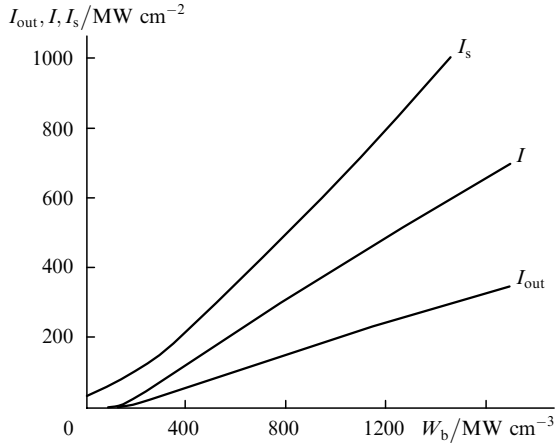

Figure 6. Dependences of the output radiation intensity I_{out}, the intracavity intensity I, and the saturating power density I_s on the specific pump power W_b in a liquid xenon laser.

It follows from the above analysis that excimer lasers operating on condensed rare gases have a unique possibility, which is absent in lasers of other types: lasing in excimers can occur both in condensed and gas phases. In this case, laser action can take place at one or several adjacent frequencies. Recall that the luminescence bands of xenon excimers in all aggregate states are overlapped. Let us assume as a reasonable estimate that Xe_2^* excimers in the gas phase can emit laser radiation up to the temperature 1000 K. Then, having rapidly deposited a specific pump energy of 500 J cm^{-3} to a crystalline xenon at temperature close to zero, which rises its temperature to 1000 K, we see that the specific energy output can be in principle of the order of 100 J cm^{-3}. Such large specific pump energies can be obtained upon nuclear pumping, which was considered in [28] as applied in semiconductor lasers. The efficiency of spontaneous emission of excimers is, as rule, higher than that upon lasing. Therefore, it seems promising to consider systems with nuclear pumping of condensed rare gases as powerful VUV sources of spontaneous or amplified spontaneous emission without the use of mirrors.

5. Conclusions

As follows from the above calculations, the first liquid xenon excimer laser was simultaneously the first gas excimer laser. The remarkable optical properties of condensed rare gases combine the properties of semiconductors and gases. Therefore, it is not by chance that the selected way of advanced development to the wide-energy-gap semiconductor lasers initiated in the mid-1960s resulted in the creation of excimer lasers operating simultaneously in condensed and gas phases. The behaviour of condensed rare gases at high specific pump powers and low temperatures remains poorly studied so far. In semiconductors under such conditions, electron – hole drops are formed [29], while these effects have not been studied in condensed rare gases up to now. Condensed rare gas lasers produce high specific output powers, exceeding 1 J cm^{-3}, which was demonstrated already for the first excimer laser. The principal possibility of the uninterrupted operation of these lasers upon crystal – liquid – gas phase transitions can result in the increase in the output power almost by two orders of magnitude. The creation of the first excimer laser, in realisation of which the role of N.G. Basov was crucial, opened up the way to the development of high-power efficient VUV lasers. Recent studies show that the possibilities of applications of condensed rare gases as laser media are far from being exhausted.

Appendix

The system of balance equations for the concentrations of components of the active medium of a condensed xenon excimer laser can be written in the form (see [20] and Fig. 4)

$$\frac{dn_{H_1}}{dt} = W^+ - \frac{n_{H_1}}{\tau_{H_1}} + (\delta_{S_1} n_{S_1} + \delta_{T_1} n_{T_1})\, n_e + \sum_{i,j} p_{ij}\, n_i n_j + (\sigma_{S_1} n_{S_1} + \sigma_{T_1} n_{T_1} + \sigma_{H_2} n_{H_2}) i_{ph},$$

$$\frac{dn_{H_2}}{dt} = \frac{n_{H_1}}{\tau_{H_1}} - (\alpha_1 + \alpha_2) n_{H_2} n_e + (\delta_{S_2} n_{S_2} + \delta_{T_2} n_{T_2}) n_e + \sum_{i,j} p_{ij}\, n_i n_j + (\sigma_{S_2} n_{S_2} + \sigma_{T_2} n_{T_2} - \sigma_{H_2} n_{H_2}) i_{ph},$$

$$\frac{dn_{S_1}}{dt} = W^* - \frac{n_{S_1}}{\tau_{S_1}} + (\alpha_1 n_{H_2} - \delta_{S_1} n_{S_1} + k_{T_1} n_{T_1} - k'_{T_1} n_{S_1} - q_{S_1} n_{S_1}) n_e - \sum_j p_{S_1 j}\, n_j n_{S_1} - \sigma_{S_1} n_{S_1} i_{ph},$$

$$\frac{dn_{T_1}}{dt} = -\frac{n_{T_1}}{\tau_{T_1}} + (\alpha_2 n_{H_2} - \delta_{T_1} n_{T_1} - k_{T_1} n_{T_1} + k'_{T_1} n_{S_1} - q_{T_1} n_{T_1}) n_e - \sum_j p_{T_1 j}\, n_j n_{T_1} - \sigma_{T_1} n_{T_1} i_{ph},$$

$$\frac{dn_{S_2}}{dt} = \frac{n_{S_1}}{\tau_{S_1}} + (k_{T_2} n_{T_2} - k'_{T_2} n_{S_2} - \delta_{S_2} n_{S_2} - q_{S_2} n_{S_2}) n_e$$

$$- \sum_j p_{S_2 j} n_j n_{S_2} - \frac{n_{S_2}}{\tau_{S_2}} - (\sigma_{S_2} n_{S_2} + \sigma_0 n_{S_2}) i_{ph},$$

$$\frac{dn_{T_2}}{dt} = \frac{n_{T_1}}{\tau_{T_1}} + (k'_{T_2} n_{S_2} - k_{T_2} n_{T_2} - \delta_{T_2} n_{T_2} - q_{T_2} n_{T_2}) n_e$$

$$- \sum_j p_{T_2 j} n_j n_{T_2} - \frac{n_{T_2}}{\tau_{T_2}} - \sigma_{T_2} n_{T_2} i_{ph},$$

where $i, j = T_1, S_1, T_2, S_2$,

$$\frac{3}{2} k_B n_e \frac{dT_e}{dt} = W^+ \left(I_i - E_g - \frac{3}{2} k_B T_e \right) - \frac{3}{2} k_B \beta T_e^{1/2} (T_e - T) n_e$$

$$+ (k'_{T_1} \varepsilon_{S_1} n_{S_1} - k_{T_1} \varepsilon_{T_1} n_{T_1} + k'_{T_2} \varepsilon_{S_2} n_{S_2} - k_{T_2} \varepsilon_{T_2} n_{T_2}) n_e$$

$$- \sum_{m,r} \delta_{m_r} n_{m_r} n_e \left(\varepsilon_{H_r} - \varepsilon_{m_r} + \frac{3}{2} k_B T_e \right) + \sum_k q_k \varepsilon_k n_k n_e$$

$$+ \sum_{m,r} \sigma_{m_r} n_{m_r} i_{ph} \left(h\nu - \varepsilon_{H_r} + \varepsilon_{m_r} - \frac{3}{2} k_B T_e \right)$$

$$+ \sum_{k,l} \left(\varepsilon_k + \varepsilon_l - \frac{3}{2} k_B T_e \right) n_k n_l,$$

where the index m_r is formed from $m = T, S$ and $r = 1, 2$; and $k, l = m_r$,

$$\beta_m \frac{di_{ph}}{dt} = nc(\sigma_0 n_{S_2} - a_i - \sigma_{S_1} n_{S_1} - \sigma_{T_1} n_{T_1} - \sigma_{S_2} n_{S_2}$$

$$- \sigma_{T_2} n_{T_2} - \sigma_{H_2} n_{H_2} - a_r) i_{ph} + j_{sp},$$

$$\rho c_p \frac{dT}{dt} = W_b,$$

$$n_e = n_{H_1} + n_{H_2}.$$

Here, p_{ij} are the rate constants of quenching in collisions between excitons of the ith and jth types; q_j and δ_j are the rate constants of quenching and ionisation of excitons by electrons; τ_j, σ_j and n_j are the lifetime, the photoionisation cross section, and the exciton concentration, respectively; i_{ph} is the photon flux density; n_e and T_e are the electron density and temperature, respectively; T is the medium temperature;

$$j_{sp} = \frac{nc}{\pi} \frac{n_{S_2}}{\tau_{S_2}} \frac{\Delta\nu_{las}}{\Delta\nu_{sp}} \frac{\Delta\Omega_{las}}{4\pi}$$

is the intensity of a spontaneous emission source; $a_r = -[\ln(1/R_1 R_2)]/(2L)$ is the effective absorption coefficient of the resonator mirrors: $\alpha_1 = \alpha_2 = 0.5\alpha_0 \times (300\,\mathrm{K}/T_e)^{1/2}$ are the rate constants of dissociative recombination; $\alpha_0 = 7 \times 10^{-9}$ cm^3 s^{-1}; $n = 1.5$ is the refractive index of condensed xenon; $\beta = 4 \times 10^7$ s^{-1} K$^{-1/2}$ is the electron deceleration constant; $\beta_m = L_m/L = 4$ is the ratio of the distance L_m between mirrors to the active-region length L; $\Delta\nu_{las}/\Delta\nu_{sp} = 0.01$ is the ratio of the laser linewidth to the spontaneous emission linewidth; $\Delta\Omega_{las} = 10^{-3}$ is the solid angle of laser radiation; $\rho = 3.1$ g cm^{-3} and $c_p = 0.17$ J g^{-1} K^{-1} is the density and the specific heat of liquid xenon;$\sigma_0 = 1.5 \times 10^{-17}$ cm^2 is the stimulated-transition cross section. The rate constants δ_j of ionisation of electrons and the rate constants for transitions between the lower and upper exciton levels k_{T_1} and k_{T_2}, which depend on temperature, were calculated from expression (7) at each step of the numerical calculation. The other rate constants and cross sections for reactions are presented in Tables 1–4.

Table 1. Lifetimes/ns.

τ_{S_2}	τ_{T_2}	τ_{S_1,T_1,H_1}
2.4	27	10^3

Table 2. Energies/eV.

ε_{H_1}	ε_{H_2}	ε_{S_1}	ε_{T_1}	ε_{S_2}	ε_{T_2}
9.28	8.78	8.38	8.26	7.76	7.64

Table 3. Quenching rate constants/cm^3 s^{-1}.

q_{S_1,T_1,S_2,T_2}	$p_{S_1S_1,T_1T_1,T_1S_1}$	$p_{S_1T_2,T_1T_2,S_1S_2}$	$p_{S_2S_2,T_2S_2,T_2T_2}$
10^{-9}	10^{-7}	10^{-8}	10^{-9}

Table 4. Photoabsorption cross sections/10^{-19} cm^2.

σ_{S_1}	σ_{S_2}	σ_{T_1}	σ_{T_2}	σ_{H_2}
6	2	8	2	2

References

1. Frenkel J. *Phys. Rev.*, **37**, 17, 1276 (1931).
2. Basov N.G. *IEEE J. Quantum Electron.*, **2**, 354 (1966).
3. Basov N.G., Bogdankevich O.V., Devyatkov A.G. *Zh. Eksp. Teor. Fiz.*, **8**, 1536 (1966).
4. Jortner J., Meyer L., Rice S.A., Wilson E.G. *J. Chem. Phys.*, **42**, 4250 (1965).
5. Molchanov A.G., Poluektov I.A., Popov Yu.M. *Fiz. Tverd. Tela*, **9**, 3363 (1967).
6. Basov N.G., Bogdankevich O.V., Popov Yu.M., Danilychev V.A., Molchanov A.G., Kashnikov G.N., Balashov E.M., Lantsov N.P., Khodkevich D.D. *A Study of Emission of Condensed Noble Gases Upon Electron Excitation* (FIAN Report) (Moscow, 1969).
7. Basov N.G., Balashov E.M., Bogdankevich O.V., Danilychev V.A., Kashnikov G.N., Lantsov N.P. *J. Luminescence*, **1-2**, 834 (1970).
8. Basov N.G., Bogdankevich O.V., Danilychev V.A., Kashnikov G.N., Kerimov O.V., Lantsov N.P. *Kratk. Soobshch. Fiz. FIAN*, (7), 68 (1970).
9. Basov N.G., Danilychev V.A., Popov Yu.M., Khodkevich D.D. *Pis'ma Zh. Eksp. Teor. Fiz.*, **12**, 473 (1970).
10. Basov N.G., Danilychev V.A., Molchanov A.G., Popov Yu.M., Khodkevich D.D. *Abstract of Papers, International Conference on Luminescence* (Leningrad, 1972); *Izv. Akad. Nauk SSSR, Ser. Fiz.*, **37**, 494 (1973).
11. Molchanov A.G. Preprint FIAN, (113) (Moscow, 1971); *Kratk. Soobshch. Fiz. FIAN*, (4), 9 (1971).
12. Molchanov A.G. *Usp. Fiz. Nauk*, **106**, 165 (1972) [*Soviet Physics Uspekhi*, **15**, 124 (1972)].
13. Koehler H.E., Ferderber L.J., Redhead D.L., Ebert P.J. *Appl. Phys. Lett.*, **21**, 198 (1972).
14. Wallace S.C., Hodgson R.T., Dreyfus R.W. *Appl. Phys. Lett.*, **23**, 22 (1973).
15. Gerardo J.B., Johnson A.W. *J. Appl. Phys.*, **44**, 4120 (1973).
16. Hughes W.M., Shannon J., Kolb A., Ault E., Bhaumik M. *Appl. Phys. Lett.*, **23**, 385 (1973).
17. Huber E.E. Jr., Emmons D.A., Lerner R.M. *Opt. Commun.*, **11**, 155 (1974).

18. Bush B., Ulrich A., Krotz W., Ribitzki G. *Appl. Phys. Lett.*, **53**, 1172 (1988).
19. Loree T.R., Showalter R.R., Johnson T.M., Birmingham B.S., Hughes W.H. *Opt. Lett.*, **14**, 1051 (1989).
20. Nahme H., Schwentner N. *Appl. Phys. B*, **51**, 177 (1990).
21. Schwentner N. *J. Mol. Struct. (Netherland)*, **222**, 151 (1990).
22. Houtermans F.G. *Helv. Phys. Acta*, **33**, 933 (1960).
23. Carbone R.J., Litvak M.M. *J. Appl. Phys.*, **39**, 2413 (1968).
24. Baldini G. *Phys. Rev.*, **128**, 1562 (1962).
25. Takahashi T., Konno S., Hamada T., Miyajima M., Kubota S., Nakamoto A., Hitach A., Shibamura E., Doke T. *Phys. Rev. A*, **12**, 1771 (1975).
26. Molchanov A.G. *Trudy FIAN*, **171**, 54 (1986) [*Proc. Lebedev Phys. Inst. Series*, **171**, 75 (New York: Nova Science Publishers, 1988)].
27. Kessler T., Nahme H., Schwentner N., Dossel O. *Opt. Commun.*, **55**, 22 (1985).
28. Molchanov A.G., Popov Yu.M. *Fiz. Tverd. Tela*, **11**, 1965 (1969).
29. Keldysh L.V., in *Eksitony v poluprovodnikakh* (Excitons in Semiconductors) (Moscow: Nauka, 1971).